Research Square

Preprints are preliminary reports that have not undergone peer review.
They should not be considered conclusive, used to inform clinical practice,
or referenced by the media as validated information.

Safety Profile of a Magnetic Iron Oxide Nanoparticle-Based Device for Lens Removal: A Comparative Study with Phacoemulsification in a Rabbit Model

Tet Fah Wong

tfwongkl@gmail.com

Vision Care Solutions Sdn Bhd

Lik Voon Kiew
Norlina Ramli
Nadzariah Cheng
Haryanti Azura Mohamad Wali
Fatin Nafisah Hamzah
Nur Azmina Mohd Zailan

Article

Keywords:

Posted Date: November 6th, 2026

DOI: https://doi.org/10.21203/rs.3.rs-11581329/v1

License: This work is licensed under a Creative Commons Attribution 4.0 International License. Read Full License

Additional Declarations: There is no conflict of interest

Abstract

Background

To evaluate the ocular safety of a novel magnetic iron oxide nanoparticle-based device for lens removal compared to standard phacoemulsification.

Methods

Twelve New Zealand white rabbits were randomly assigned to either a novel device group or a phacoemulsification group with one rabbit from each group is excluded from the study. (n = S in each group), Only one eye from each rabbit was used. Scotopic and photopic electroretinogram (ERG) a-wave and b-wave amplitudes were recorded preoperatively and 4 weeks postoperatively. Corneal endothelial cell density was measured preoperatively and at 2 and 4 weeks postoperatively. Intraocular pressure (IOP) was measured preoperatively and at 1, 2, and 4 weeks postoperatively. After four weeks, the eyes were enucleated for Haematoxylin and Eosin (H & E) and Prussian blue staining of the cornea, iridocorneal angle, and sensory

1. Introduction

Cataract is the leading cause of reversible blindness worldwide [1, 2], affecting approximately 95 million people, with about 30 million cataract surgeries performed annually [3]. Introduced by Charles Kelman in 1967, phacoemulsification remains the gold standard for lens removal, offering small incisions, rapid visual recovery and excellent safety outcomes [4,5]. Nuclear fragmentation remains its most challenging step. Nuclear division manoeuvres are associated with posterior capsular tears, dropped nuclei and endothelial cell damage, particularly in eyes with small pupils, hard nuclei, shallow anterior chambers or unstable lenses [6,7,8]. Devices and techniques developed to reduce these complications include manual choppers, mechanical looping devices and femtosecond lasers [9,10]. We developed a readily manoeuvrable lens removal device that combines a pulsed magnetic probe with an iron oxide nanoparticle solution infiltrated into the nucleus. *A* low-frequency magnetic field causes the nanoparticles to vibrate, generating shear forces that alter lens fibre membranes at the micro- or nanoscale and fragment the nucleus. Li W et al. reported a similar effect in their study, in which a low-frequency pulsed magnetic field applied to magnetic nanoparticles caused structural collapse within tumour masses [11].

Iron oxide nanoparticles are used as magnetic resonance imaging contrast agents and for parenteral iron replacement therapy [12, 13]. Ferumoxytol, an iron oxide nanoparticle formulation for intravenous infusion, was selected for intraocular use in this study because of its safety profile in humans and biocompatibility [14].

The eye has several barriers to nanoparticle clearance, including the corneal endothelium, trabecular meshwork and blood-retinal barrier. Nanoparticles injected into the anterior chamber may accumulate in the trabecular meshwork, obstruct aqueous outflow and elevate intraocular pressure. Those reaching the posterior segment may deposit in the retina, where iron overload can cause oxidative stress, lipid peroxidation and photoreceptor degeneration [15,16]. Iron oxide nanoparticle-based intraocular devices therefore require rigorous ocular safety evaluation before clinical translation. Rabbits are widely used in preclinical ophthalmic safety studies because of their large eyes, well-characterised anatomy and surgical responses similar to those of humans [17].

-

We evaluated the ocular safety of the novel magnetic iron oxide nanoparticle-based lens removal device against standard phacoemulsification in a rabbit model. Outcomes included corneal endothelial cell density, scotopic and photopic ERG a- and b-wave amplitudes, intraocular pressure, and histopathological assessments of the cornea, iridocorneal angle and sensory retina, with Prussian blue staining for iron deposition. We hypothesized that the device would preserve retinal function while providing corneal endothelial, intraocular pressure and histopathological safety equivalent to phacoemulsification.

2. Materials and Methods

The Institutional Animal Care and Use Committee (IACUC) of the Faculty of Medicine, University of Malaya, approved the animal-use protocol, including use of the novel device and intraocular ferumoxytol. The study was conducted in accordance with the ARVO Statement for the Use of Animals in Ophthalmic and Vision Research.

2.1 Animals

Twelve New Zealand white rabbits aged 5 months and weighing 4–5 kg were randomly allocated equally to the novel device and phaco groups. One rabbit in the phaco group was excluded from the study because of a congenital defect; one in the novel device group was excluded from statistical analysis because of posterior capsule rupture. Only one eye per rabbit was used.

2.2 Novel Device and Ferumoxytol Solution

The device comprised a handpiece with a needle probe and a pulse power supply that generated pulsed magnetic flux, delivered through the needle to the nuclear surface.

A 0.0012% ferumoxytol solution was prepared by adding 0.2 mL of 3% ferumoxytol to 500 mL of balanced salt solution.

2.3 Surgical Procedures

Thirty minutes before surgery, pupils were dilated with topical tropicamide 1% and phenylephrine 2.5%. Rabbits were dark-adapted for 30 min in a holding room, then anaesthetised by intramuscular injection of xylazine (3 mg/kg) and ketamine (30 mg/kg). Slit-lamp examination and specular microscopic endothelial cell counts were followed by electroretinography (ERG) and intraocular pressure (IOP) measurements.

After preoperative data collection, general anaesthesia was maintained with 2% inhaled isoflurane. The same surgeon operated on all rabbits using standard aseptic techniques.

-

All rabbits received 2.6 mm corneal incisions, and AJL Vise 2% ophthalmic viscosurgical device (OVD) material was used in both groups. Continuous curvilinear capsulorhexis was performed with an Oertli radiofrequency capsulorhexis needle. Before hydrodissection, the nuclear surface was grooved with a phaco handpiece needle probe to facilitate nanoparticle penetration. Hydrodissection with 2–5 mL of 0.0012% ferumoxytol solution loosened the nucleus from the capsular bag. The novel device needle was inserted into the OVD-maintained anterior chamber. Pulsed magnetic flux (5 V, 400–500 Hz, 60% duty cycle, 1.5-2 mT) was applied to the nuclear surface. As the nucleus softened, the needle tip was moved from the periphery towards the centre until the entire

nucleus fragmented. Fragments were aspirated with minimal phaco power using the Alcon Laureate Phaco System. The remaining cortex and OVD were removed by irrigation/aspiration (I/ A), and the incision was closed with a single

10 – 0 nylon stitch. Tobramycin, dexamethasone, timolol 0.5% and moxifloxacin 0.5% eye drops were administered at the end of surgery.

The phaco group underwent similar procedures, except that balanced salt solution (BSS) was used for hydrodissection and nuclei were divided and removed using the divide-and-conquer technique. Postoperatively, tobramycin, dexamethasone and moxifloxacin 0.5% eye drops were administered four times daily for 4 weeks. Timolol 0.5% eye drops were added twice daily if postoperative assessments showed elevated IOP.

At 4 weeks postoperatively, all rabbits were euthanised with an overdose of intravenous pentobarbital sodium (100 mg/kg). Their eyes were enucleated and preserved in 10% neutral buffered formaldehyde for histopathological analysis.

2.4 Post-Operative Assessment

All post-operative assessments were performed with the animals fully sedated using intramuscular Xylazine (3 mg/kg) and Ketamine (30 mg/kg).

2.4.1 Corneal Endothelial Cell Density

A CSM SUOER SW-7000 corneal specular microscope was used to measure central corneal endothelial cell density before surgery and 2 and 4 weeks postoperatively [18).

2.4.2 Electroretinography (ERG)

Scotopic and photopic electroretinograms were recorded before surgery and 4 weeks postoperatively using the RETIport ERG and VEP systems according to rabbit-eye testing protocols. Gold-plated corneal electrodes were placed on the corneal surface, with ground electrodes near the ears. Ten flashes were used for scotopic stimulation and five for photopic stimulation.

2.4.3 Intraocular Pressure

Intraocular pressures were measured pre-operatively and at 1, 2, and 4 weeks post-operatively using an iCare Tonovet tonometer.

2.4.4 Histopathology and Prussian Blue Staining

Enucleated eyes from both groups were examined histopathologically at the Mymab Biologics Laboratory, University Putra, Malaysia. Globes were grossed to ensure clear visualisation of the cornea, iridocorneal angle and retina in tissue sections. Sections were embedded in paraffin and stained with haematoxylin and eosin (H&E); Prussian blue staining was used to assess iron deposition.

2.5 Statistical Analysis

Data were analysed using R (Version 4.X.X; R Foundation, Vienna, Austria) and SPSS (Version 27; IBM Corp., Armonk, NY, USA). Continuous variables were reported as mean ± standard deviation (SD). Paired and independent t-tests were used for within-group and between-group comparisons, respectively. Wilcoxon signed-

rank and Mann-Whitney U tests were used for nonparametric sensitivity analyses. Statistical significance was set at $p < 0.05$.

3. Results

The final analysis included five rabbits per group (n = 5). Slit-lamp examination showed minimal anterior chamber inflammation in all eyes. Corneal oedema resolved by 14 days postoperatively in most eyes. Corneal oedema prevented specular microscopy during this period.

3.1 Analysis of Corneal Endothelial Cell Density

Table 1 presents mean central corneal endothelial cell densities at each time point for both groups. Neither group showed significant within-group changes (all $p > 0.05$), although cell counts tended to decrease at 2 weeks in the novel device group ($p = 0.075$). Between-group comparisons were performed preoperatively and at 2 and 4 weeks postoperatively; Table 1 summarises the results. The groups did not differ significantly at any time point (all $p > 0.05$). Overall, the findings suggest transient endothelial cell loss at 2 weeks with partial recovery at 4 weeks after both techniques, but no statistically significant lasting reduction in corneal endothelial cell density.

Table 1
Mean Corneal Endothelial Cell Density: Between-Group Comparisons Using Independent t-tests and Mann-Whitney Tests

Time Point	Novel Mean (SD)	Phaco Mean (SD)	Difference	t-value	p-value	Significance	Mann-Whitney P-value	Significance
Pre-op	2779.20 {107.H)	2870.00 (194.58).	-90.80	-0.91	0.39	No	0.31	No
2wk	2129.80 (627.66)	2464.40 (876.47)	-334.60	-0.69	0.51	No	0.69	No
4wk	2763.6 0 (611.94)	. 2438.00 (847.90)	+ 325.60	0.69	0.51	No	0.69	No

3.2 Electroretinogram (ERG) Analysis

3.2.1 Statistical Analysis of Scotopic ERG

Table 2 presents preoperative and postoperative mean scotopic a- and b-wave amplitudes and paired t-test results for within-group comparisons. Neither group showed significant changes in either amplitude, although the novel device group showed a trend towards increased b-wave amplitude ($p = 0.12$).

Table 3 presents between-group comparisons. Postoperative b-wave amplitude was significantly higher in the novel device group than in the phaco group (115.84 ± 23.84 μV vs 80.82 ± 7.84 μV; $p = 0.02$; Mann-Whitney $p = 0.03$).

Table 2
Mean Preoperative and Postoperative Scotopic and Photopic a- and b-wave Amplitudes: Within-Group Comparisons Using Paired t-tests and Wilcoxon Tests

Adaptation	Group	Wave	Pre-Mean µV (SD)	Post-Mean µV (SD)	Mean Change µV	t-value	p-value	Significance	Non-parametric p
Scotopic	Novel	a	13.53 (9.98)	26.51 (27.81)	+ 12.98	0.96	0.39	No	0.63 (Wilcoxon)
Scotopic	Novel	b	95.46 (8.77)	115.84 (23.84)	+ 20.38	2.00	0.12	No (trend)	0.13 (Wilcoxon)
Scotopic	Phac0	a	9.14 (2.44)	11.71 (13.40)	+ 2.57	0.44	0.68	No	0.81 (Wilcoxon)
Scotopic	Phaco	b	71.76 (11.90)	80.82 (7.84)	+ 9.06	1.68	0.17	No	0.31 (Wilcoxon)
Photopic	Novel	a	10.88 (5.25)	16.48 (8.24)	+ 5.60	1.37	0.24	No	0.31 (Wilcoxon)
Photopic	Novel	b	99.66 (10.73)	109.94 (14.71)	+ 10.28	1.31	0.26	No	0.31 (Wilcoxon)
Photopic	Phaco	a	8.01 (4.42)	16.30 (7.72)	+ 8.29	2.27	0.08	No (trend)	0.13 (Wilcoxon)
Photopic	Phaco	b	68.00 (21.70)	85.16 (11.92)	+ 17.16	1.41	0.23	No	0.31 (Wilcoxon)

Table 3
Between-Group Comparisons of Scotopic and Photopic ERG Using Independent t-tests and Mann-Whitney Tests

Adaptation	Comparison	Wave	Novel Mean µV (SD)	Phaco Mean µV (SD)	p-value	Significance	Mann - Whitney
Scotopic	Post-op	a	26.51 (27:81)	11.71 (13.40)	0.31	No	0.84
Scotopic	Post-op	b	115.84 (23.84)	80.82 (7.84)	0.02	Yes	0.03
Scotopic	*Δ* (Post-Pre)	a	+ 12.98, (30.22)	+ 2.57 (13,09)	0.50	No	0.84
Scotopic	Δ (Post-Pre)	b	+ 20.38 (22.81)	+ 9.06 (12.05)	0.36	No	0.42
Photopic	Post-op	a	16.48 (8.24)	16.30 (7.72)	0.97	No	0.84
Photopic	Post-op	b	109.94 (14.7:).)	85.16 (11.92)	0.02	Yes	0.03
Photopic	Δ (Post-Pre)	a	+ 5.61 (9.17)	+ 8.30 (8.17)	0.64	No	0.84
Photopic	*Δ*(Post-Pre)	b	+ 10.28 (17.55)	+ 17.16 (26.84)	0.65	No	0.84

3.2.2 Statistical Analysis of Photopic ERG

Table 2 presents mean photopic a- and b-wave amplitudes for both groups and paired t-test comparisons of preoperative and postoperative values. Neither group showed significant within-group changes, although a-wave amplitude tended to increase in the phaco group ($p = 0.08$). Between-group comparisons (Table 3) showed significantly higher postoperative b-wave amplitude in the novel device group than in the phaco group (109.94 ± 14.71 µV vs 85.16 ± 11.92 µV; $p = 0.02$; Mann-Whitney $p = 0.03$).

3.2.3 Summary of scotopic and photopic ERG findings

Changes from baseline (Δ = post-pre) in scotopic and photopic a- and b-wave amplitudes did not differ significantly between the novel device and phaco groups. A-wave amplitudes also showed no significant between-group differences under either condition (all $p > 0.05$). However, b-wave amplitudes were significantly higher in the novel device group under both conditions.

3.3 Intraocular Pressures Analysis

IOP was measured before surgery and at 1, 2 and 4 weeks postoperatively. Table 4 summarises mean IOP in the novel device and phaco groups. Neither group showed significant within-group IOP changes, although the novel device group showed a trend towards an IOP spike at 1 week ($p = 0.065$).

Between-group comparisons (Table 4) showed lower preoperative IOP in the novel device group than in

the phaco group (15.40 ± 0.89 vs 17.80 ± 1.10 mm Hg; p = 0.005), indicating a baseline imbalance. Postoperative differences were not significant (1 week, p = 0.83; 2 weeks, p = 0.29; 4 weeks, p = 0.39).

Nonparametric tests corroborated these findings, suggesting transient early postoperative IOP fluctuations with both techniques but no significant lasting between-group differences.

Table 4
Mean Intraocular Pressure and Between-Group Comparisons Using Independent t-tests at Each Time Point

Time Point	Novel Mean mmHg (SD)	Phaco Mean mm Hg (SD)	Mean Difference	t-value	· p-value	Non-parametric test Mann-Whitney
Pre-op	15.40 (0.89)	17.80 (1.1Q)	-2.40	-3.79	0.005	0.016
1 week	22.00 (5.39)	20.20 (16.8'6).	+ 1.80	0.22	0.830	0.840
2 weeks	14.80 (5.63)	22.00 (_12.86)	-7.20	-1.13	0.290	0.310
4weeks	20.00 (8;34)	27.40 (15.55)	-7.40	-0.92	0.390	0.420

3.4 Histopathological Findings

A histopathologist blinded to the surgical procedures reviewed the ocular histology. Figure 1A-C shows the cornea, iridocorneal angle and sensory retina of eyes in the novel device group.

3.4.1 Cornea

The Haematoxylin and Eosin staining showed normal corneal architecture in both groups, with intact epithelium, organised stromal lamellae, and a continuous endothelial monolayer. No endothelial cell apoptosis was observed in the novel device group, whereas mild apoptosis was observed in the phaco group. Prussian blue staining was negative throughout the cornea in both groups, with no detectable iron deposit in the epithelium, stroma, and endothelium. Neither group showed inflammatory cell infiltrates in any corneal layers.

3.4.2 Iridocorneal Angle

H & E staining showed normal trabecular meshwork architecture in both groups, with no inflammatory cell infiltration, fibrosis, or pigment dispersion. Prussian blue staining was negative in the trabecular meshwork and surrounding tissues in both groups, confirming no iron accumulation in the aqueous outflow pathway.

3.4.3 Sensory Retina

Retinal sections from both groups showed preserved laminar organisation, distinct nuclear layers and ganglion cells, and intact inner and outer photoreceptor segments, with no cell loss, vacuolisation or inflammatory infiltration. Prussian blue staining was negative throughout the sensory retina, including the ganglion cell, inner nuclear and outer nuclear layers and photoreceptor segments.

4. Discussion

-

Hemalatha et al. found little or no toxicity to retinal structure, endothelial cells, photoreceptor function or aqueous drainage after intravitreal or anterior chamber magnetic nanoparticle (MNO) injections in Sprague-Dawley rats, suggesting intraocular safety [19). Our nanoparticle-based device preserved inner retinal function (ERG b-wave) significantly better than phacoemulsification, with equivalent corneal endothelial safety, stable intraocular pressure and normal ocular histology. Prussian blue staining

confirmed no iron deposition in the cornea, trabecular meshwork or sensory retina at 4 weeks postoperatively.

4.1 Corneal Endothelial Cell Safety

Corneal endothelial cell density did not differ significantly between groups (preoperative, p = 0.39; 2 and 4 weeks, p = 0.51 each). Both showed transient cell loss at 2 weeks with partial recovery after 4 weeks, consistent with reported losses of 4–25% at 1–3 months after phacoemulsification [20). This suggests surgical trauma and postoperative inflammation rather than device-specific toxicity. The novel device caused no greater loss at any time point, indicating no additional endothelial risk from nanoparticles or their manipulation. Preserved corneal architecture on H&E staining supports the specular microscopic findings.

4.2 Retinal Safety: Functional and Structural Preservation

Postoperative b-wave amplitudes were significantly higher with the novel device than with phacoemulsification under scotopic (115.84 ± 23.84 μV vs 80.82 ± 7.84 μV; p = 0.02) and photopic (109.94 ± 14.71 μV vs 85.16 ± 11.92 μV; p = 0.02) conditions. The b-wave reflects ON-bipolar and Muller glial cell activity [21), which is highly sensitive to metabolic, ischaemic and mechanical trauma [22). Its preservation suggests less inner retinal stress with the nanoparticle-based approach. H&E staining corroborated the ERG findings, showing intact retinal layers and inner and outer photoreceptor segments. The undamaged inner nuclear layer, containing bipolar cell bodies, supports their functional preservation. Together, these findings suggest favourable functional and structural retinal safety.

4.3 Intraocular Pressure Safety

Both groups had transient IOP spikes at 1 week, with means approaching baseline by 2 weeks. Postoperative between-group differences were nonsignificant (1 week, P = 0.83; 2 weeks, P = 0.29; 4 weeks, P = 0.39). Lower baseline IOP in the novel device group (15.4 ± 0.89 vs 17.80 ± 1.10 mm Hg; p = 0.005) represents a study limitation. The transient spikes are consistent with postoperative inflammation, retained viscoelastic material or temporary trabecular obstruction, common after intraocular surgery [23). In the novel device group, no sustained IOP elevation, normal trabecular architecture on H and E staining and negative iridocorneal angle Prussian blue staining are reassuring, suggesting that nanoparticles neither obstructed aqueous outflow nor induced fibrosis.

4.4 Absence of Iron Deposition: A Critical Safety Finding

The main theoretical concern is that magnetic iron oxide nanoparticles may accumulate in ocular tissues, causing oxidative stress, inflammation or long-term toxicity [24,25].

-

At 4 weeks postoperatively, Prussian blue staining revealed no detectable iron deposits in the cornea, trabecular meshwork or sensory retina. We believe most iron oxide nanoparticles were removed during cortex removal. These negative staining results support the functional and structural findings in these tissues.

5. Limitations

Despite favourable outcomes, this study has limitations. First, the small sample (n = 5 per group) reduces statistical power and increases the risk of Type II errors. Second, the unequal baseline IOP between groups complicates interpretation of IOP results. Third, without corneal immunohistochemistry for apoptosis, low levels of apoptotic changes cannot be excluded despite preserved histomorphology on H & E staining. Fourth, the 4-week follow-up was relatively short for evaluating long-term nanoparticle safety. Finally, differences in ocular size, anatomy, and immune response between rabbits and humans may limit the findings' applicability to humans.

6. Conclusion

The magnetic iron oxide nanoparticle-based device showed favourable ocular safety in this rabbit model. Compared with phacoemulsification, the device significantly better-preserved inner retinal function (ERG b-wave), with equivalent corneal endothelial safety, stable intraocular pressure, and normal ocular histology. Prussian blue staining confirmed no iron deposition in the cornea, trabecular meshwork, or sensory retina. These results support further development of the technology and investigation in larger cohorts and human clinical trials.

Declarations

7. Conflicts of interest

T F Wong discloses that he invented the novel device, for which patent approval is pending. The authors declare no conflicts of interest concerning the publication of this article.

11. AI statement

No generative AI was used by the authors to draft, translate, summarize, or produce manuscript text, references, images, or other content.

8. Funding

The project was supported by internal self-funding.

9. Author contributions

T F Wong designed the protocol, performed the surgery and wrote the report. L V Kiew advised on magnetic nanoparticle pharmacology and revised the manuscript. N Cheng performed ERG,

10. Acknowledgements

The authors thank S H Kok, Clement K M Khoo, and M Akmal for technical assistance, and Miss WW Pok for assistance with the surgical procedures.

12. Data Availability

Data for the analyses in this study are available from the corresponding author upon reasonable request.

References

[1] Lin L, Liang Y, Hang G, Gan Q. Yang T, Liao P, Lixia Lin et al. Global, regional and national burden of cataract: A comprehensive analysis and projections from 1990 to *2021.PLoS* One 20(6): e0326263 (2025). doi: 10.1371/journal.pone.0326263

(2] Bourne RR, Stevens GA, White RA Smith IL, Flaxman SR, Price H. Causes of vision loss worldwide, 1990-2010: a systematic analysis. *Lancet Glob Health.* 2013;1(6): e339-e349 (2013)

Hashemj H,Fayaz F,Hashemi A, Khabazkhoob, M Hassan Hashei. Global prevalence of cataract surgery.

*Current Opinion in Ophthalmolmogy.*36(1); p,10-17, January (2025).doi; 10,1097/ICU0000000000001092.

Kelman CD. Phaco-emulsification and aspiration: a new technique of cataract removal. *Am J Ophthalmol*

1967;64(1):23-35 (1967).

[5] Linebarger El, Hardten DR, Shah GK, Lindstrom RL. Phacoemulsification and modern cataract surgery. *Surv Ophthalmol.* 1999;44(2): L123-147(1999).

[6] Mencuccj R, Ponchjettj C, Virgili G Gjansanti F. Corneal endothelial damage after cataract surgery. Journal of Cataract & Refractive Surgery. 2020;46(5):704–711(2020).

[7] Tajurisah I, Reddy S C. Dropped nucleus following phacoemulsification cataract surgery. *Medical J Malaysia.*

Vol.62 (5):364-367(2007).

[8) Mohammad-Rabei, Nikkhah H,Rajavi Z, Hatamj M, Haghparast M, Esfandiari H, Hossein Mohammad . Incidence and risk factors for intraoperative complications in resident-performed phacoemulsification surgery. J *Ophthalmic Vis* Res. 2025 Jul 21;20:10:18502/jovr. 120./4823 doi:10.18502/jovr.20.14823 (2025).

Hu EH, Buie T, Jensen RI, Wu D. Pamnani RD, Comparative study of safety outcomes following nucleus disassembly with and without the miLoop lens fragmentation device during cataract surgery. Clin Ophthalmol. 2022 Aug 2;16:2391-2401(2022). doi:10.2147/OPTH.5370290.

Yan Q, Han B,.Ma ZC, Quan Yan et al. Femtosecond Laser-Assisted Ophthalmic Surgery: From Laser Fundamentals to Clinical Application. *Micromachines Basel J.* 2022 Sep 30;13(10):1653(2023) doi:10.3390/mil3101653.

Li W Liu Y, Qian Z. Yang Y. Weitao Li. Yangyang Liu et al. Evaluation *of* tumor treatment of magnetic nanoparticles driven by extremely low frequency magnetic *field. scientific report Sci Rep* 7. Article number: 46287 (2017).

Peter Reimer, Thomas Balzer. Ferucarbotran (Resovist): a new clinically approved RES-specific contrast agent for contrast-enhanced MRI of the liver; properties. clinical development,and applications. *Eur Radiol.* 2003 Jun;13(6):l266-1276(2003).. doi:10.1007/s00330-002-1721-7.

Provenzano R. Schiller B. Rao M. Coyne D. Brenner L. Pereira BI, Robert Provenzano. Brigitte Schiller et al. Ferumoxytol as an intravenous iron replacement therapy in hemodialysis patients. Clin J Am Nephrol, 2009 Feb;4(2):386-393(2009). doi:10.2215/CJN.02840608.Epub 2009 Jan 28.

(14) Anzai Y. et al. Iron oxide nanoparticles: a review of their clinical applications. *Top Magn Reson*

Imaging.2003;14(2):121-130..(2003).

He X, et al. Iron overload in the retina: mechanisms and therapeutic implications. Prog *Retin Eye Res.*

2019;70:1-22 (2019).

Dunaief JL. Iron induced oxidative damage as a potential factor in age-related macular degeneration. *Exp Eye Res.*

2006;82(4):574-580 (2006).

Gwon A. The rabbit eye as a model for ophthalmic research. J *Toxicol* Pathol.2008;21(3):123-128(2008).

McCarey BE, et al. Specular microscopy of corneal endothelium. *Arch. Ophthalmol.* 2008;126 10:77-82 (2008).

Raju HB,Hu Y, Vedula A, Dubovy SR, Goldberg JL, Hemalatha et al. Evaluation of Magnetic Micro- and Nanoparticle Toxicity to Ocular Tissues. *PLoS One, Vol 6(5) pp. e17452-e17452* (2011). doi :https://doi.org/10.1371/journal.pone00l7452.

Walkow T, Anders N, Klebes. Endothelial Cell Loss After Phacoemulsification: relation to preoperative and intraoperative parameters.J Cataract Refract Surg. 2000;26(5):727-732.

Stockton RA. Slaughter MM. B-wave of the electroretinogram: a reflection of ON bipolar cell activity.*J Gen Physiol*

93, 101-122 (1989).

Augustin AJ, Dick HB. Oxidative tissue damage after phacoemulsification: influence of ophthalmic viscosurgical devices. J Cataract *Refract Surg.* 2004;30(2):424-427. (2004).

Shingleton BJ, Pasternack JJ, Hung JW, O'Donoghue MW, Singleton BJ, et al. Intraocular pressures after phacoemulsification. J *Cataract Refract Sur9.* 2000;26(6):862-866(2000)

Soenen SJ, Rivera-Gil P, Montenegro JM,Parak WI, De Smedt SC, Braeckmans K, Soenen SJ et al. Cellular toxicity of inorganic nanoparticles: common aspects and guidelines for improved nanotoxicity evaluation. Nano Today. 2011;6(5):446-46S (2011).

[25] Sharifi S, Behzadi S, Laurent S, Laird Forrest M, StroeveP,Mahmoudi M,Sharifi S, et al. Toxicity of nanomaterials.

Chem Soc Rev. 2012; 41(6):2323-2343..(2012)

Figures

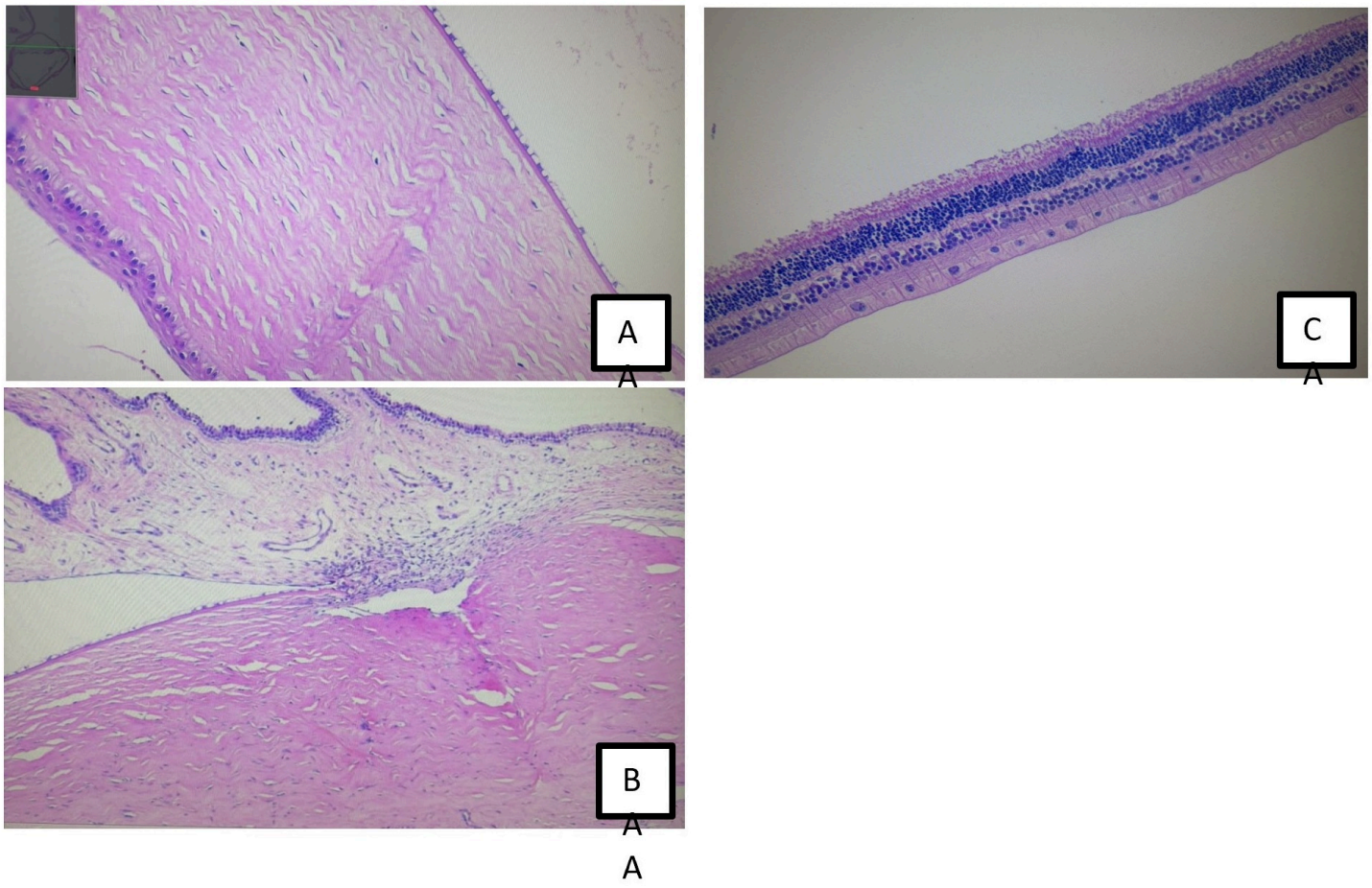


Figure 1

H & E Staining of Cornea (A), Iridocorneal Angle (B), H & E Staining of Retina (C)